

TABLE OF CONTENTS

Section	Page
1 INTRODUCTION	1
1.1 The Standard Model and the Electroweak Interaction	1
1.2 The Q-weak Experiment	3
1.3 Inelastic Parity Violating Asymmetry	6
1.3.1 The Δ Resonance	7
1.3.2 Formalism and Measurement	8
1.4 The Beam Normal Single Spin Asymmetry	8
1.5 Inelastic Beam Normal Single Spin Asymmetry	9
1.6 Thesis Outline	9
2 THEORY	10
2.1 Electron Scattering Beyond the Born Approximation	10
2.1.1 2-photon Exchange	11
2.2 Experimental Observation of Beam Spin Asymmetry	12
2.2.1 Measurement of the Beam Normal Single Spin Asymmetry	13
2.2.2 Imaginary Part of Two-photon Diagram	15
2.3 The $\gamma^* \Delta\Delta$ Form Factors	15
2.4 Model Calculations	16
2.5 Goals of the Inelastic Transverse Physics Program	17
3 DISCUSSION AND CONCLUSIONS	19
3.1 Summary of Results	19
3.2 Contribution Towards Q-weak Experiment	19
3.2.1 Beam Modulation	19
3.2.2 Beamline Work	20

Section	Page
3.2.3 Beam Normal Single Spin Asymmetry in Inelastic e+p Scattering	21
REFERENCES	22

SECTION 1

INTRODUCTION

The Q-weak experiment at the Thomas Jefferson National Accelerator Facility, USA, (TJNAF or JLab) is aimed to measure the weak charge of the proton by measuring parity-violating asymmetry of elastic electron-proton scattering at low four-momentum-transfer squared (Q^2). The weak charge of the proton in the Standard Model (SM) is suppressed and any observed deviations from the SM predictions found in this high precision measurement will suggest signatures of new physics.

1.1 The Standard Model and the Electroweak Interaction

The development of the SM in the twentieth century is one of the greatest achievements of the particle physics which is a theory concerning the electromagnetic, weak, and strong nuclear interactions [1]. The SM states that the fundamental particles that make up all matter are quarks and leptons, and that they interact through the strong, weak, and electromagnetic fundamental interactions by exchanging force carrier particles. A summary of the SM particles with their mass, charge, and spin is shown in Figure 1.1. The weak interaction is unique among the four known forces, because it is the only force known to violate parity. A parity transformation is defined as a discrete change of spatial coordinates from (x, y, z) to $(-x, -y, -z)$. The electromagnetic and weak interactions have been unified in an electroweak theory is one of several successes of the SM. The Prescott experiment [2] at the Stanford Linear Accelerator Center (SLAC) first experimentally confirmed SM predictions of the weak neutral current [3–5] by measuring parity violating asymmetry in deep inelastic electron-deuteron scattering. Over the past half-a-century, the general structure of the SM was confirmed by many experiments.

Despite the many successes, there are also many reasons why the SM is not a complete theory. The missing phenomena from the SM are dark matter, dark energy, gravity, etc. The recently observed 3σ deviation of the anomalous magnetic moment of muon [7] at Brookhaven National Laboratory could also be related to new physics extensions beyond the SM. The SM falls short of being a complete theory of fundamental interactions, one of them being parity violation. The SM incorporates parity violation by expressing the weak interaction as a chiral gauge interaction.

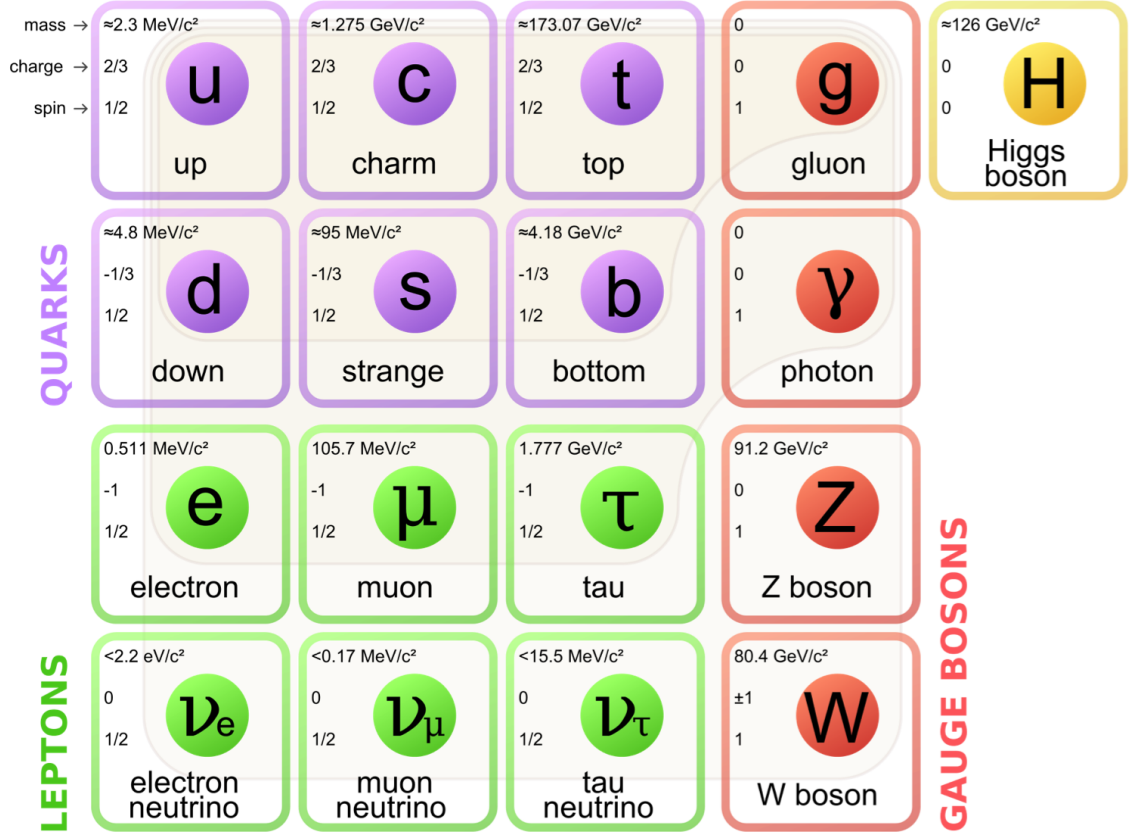


Figure 1.1 The Standard Model of elementary particles [6]. The three generations of matter, gauge bosons are shown in the fourth column, whereas the newly discovered Higgs boson in the fifth.

Over last couple of decades, parity-violating electron scattering (PVES) has become an important experimental tool to investigate the contribution of the quark-antiquark sea of the nucleon to its electromagnetic structure. The advanced technologies and improved experimental techniques allowed us to do challenging parity-violating experiments to measure of the parity-violating asymmetries at the parts-per-billion level. Figure 1.3 shows a brief history of the measured asymmetry in different PVES experiments. The difficulty level of an experiment increases with the decrease of the size and precision of the asymmetry. As shown in the Figure, the Q-weak experiment is expected to measure the most precise value of the PV asymmetry in e+p scattering to date.

Table 1.1 The electric and weak charges of elementary particles in the Standard Model.

Particle	EM Charge	Weak Charge		
u	2/3	$-2C_{1u}$	$1 - (8/3)\sin^2 \theta_W$	$\sim 1/3$
d	1/3	$-2C_{1d}$	$1 - (8/3)\sin^2 \theta_W$	$\sim 1/3$
p (uud)	1	$-2(2C_{1u} + C_{1d})$	$1 - 4\sin^2 \theta_W$	~ 0.07
n (udd)	0	$-2(2C_{1u} + C_{1d})$		~ 1

1.2 The Q-weak Experiment

The SM makes a firm prediction of the weak charge of the proton (Q_W^p), based on the running of the weak mixing angle $\sin^2 \theta_W$ from the Z^0 pole down to low energies. Any significant deviation of $\sin^2 \theta_W$ from the SM prediction at low Q^2 would be a signal of new physics, whereas agreement would place new and significant constraints on possible SM extensions. The weak charge of the proton is suppressed in SM (as shown in Table 1.1) and a precise measurement of the quantity will challenge the SM predictions and search for new physics.

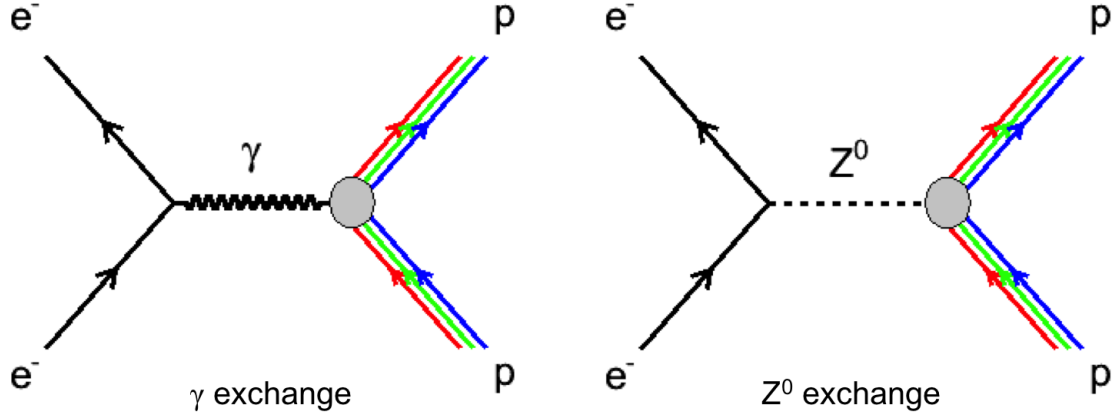


Figure 1.2 The Feynman diagrams for the parity conserving and parity violating semileptonic electroweak interactions.

The electron-proton scattering can involve either an exchange of a photon or a Z^0 boson (Figure 1.2). The scattering cross section is a summation and an interference of the two invariant amplitudes.

$$\sigma \approx |\mathcal{M}_{EM} + \mathcal{M}_{weak}|^2 \approx |\mathcal{M}_{EM}|^2 + 2\Re \mathcal{M}_{EM}^* \mathcal{M}_{weak} + |\mathcal{M}_{weak}|^2, \quad (1.2.1)$$

Here \mathcal{M}_{EM} , and \mathcal{M}_{weak} are the amplitudes for the exchange of a photon and Z^0 boson respectively. The sign of \mathcal{M}_{weak} changes the sign of the interference term under a parity transformation. Experimentally, this is achieved by changing the helicity of a longitudinally polarized electron scattering from an unpolarized nucleon. The parity-violating asymmetry is then defined as

$$A_{PV} = \frac{\vec{\sigma} - \bar{\vec{\sigma}}}{\vec{\sigma} + \bar{\vec{\sigma}}}, \quad (1.2.2)$$

where $\vec{\sigma}(\bar{\vec{\sigma}})$ is the cross section for the electrons scattering with spin polarized parallel (anti-parallel) to their direction of motion. Given that $|\mathcal{M}_{weak}| \ll |\mathcal{M}_{EM}|$, this asymmetry reduces to being proportional to

$$A_{PV} \sim \frac{2\mathcal{M}_{weak}\mathcal{M}_{EM}}{|\mathcal{M}_{EM}|^2}. \quad (1.2.3)$$

At tree level, the full form of the asymmetry for electron-proton scattering can be written as [8]

$$A_{PV} = \left[\frac{-G_F Q^2}{4\sqrt{2}\pi\alpha} \right] \left[\frac{\varepsilon G_E^{p\gamma} G_E^{pZ} + \tau G_M^{p\gamma} G_M^{pZ} - (1 - 4\sin^2 \theta_W) \varepsilon' G_M^{p\gamma} G_A^e}{\varepsilon (G_E^{p\gamma})^2 + \tau (G_M^{p\gamma})^2} \right], \quad (1.2.4)$$

where the Fermi constant is denoted by G_F . The kinematic factors in terms of proton mass M , scattering angle θ , and four-momentum transfer squared Q^2 are given by

$$\varepsilon = \frac{1}{1 + 2(1 + \tau) \tan^2 \frac{\theta}{2}}, \varepsilon' = \sqrt{\tau(1 + \tau)(1 - \varepsilon^2)}, \tau = \frac{Q^2}{4M^2}, \quad (1.2.5)$$

and electromagnetic form factors can be expressed as

$$G_{E,M}^{pZ} = (1 - 4\sin^2 \theta_W) G_{E,M}^{p\gamma} - G_{E,M}^{n\gamma} - G_{E,M}^s. \quad (1.2.6)$$

The weak charge of the proton in the SM is given by

$$Q_W^p = (1 - 4\sin^2 \theta_W). \quad (1.2.7)$$

Defining

$$A_0 = \frac{-G_F Q^2}{4\sqrt{2}\pi\alpha}, \quad (1.2.8)$$

and using equations 1.2.4, 1.2.5, 1.2.6, 1.2.7, the reduced asymmetry can be written as

$$\frac{A_{PV}}{A_0} = \left[\frac{\varepsilon G_E^{p\gamma} (Q_W^p G_E^{p\gamma} - G_E^{n\gamma} - G_E^s) + \tau G_M^{p\gamma} (Q_W^p G_M^{p\gamma} - G_M^{n\gamma} - G_M^s) - (1 - 4 \sin^2 \theta_W) \varepsilon' G_M^{p\gamma} G_A^e}{\varepsilon (G_E^{p\gamma})^2 + \tau (G_M^{p\gamma})^2} \right] \quad (1.2.9)$$

$$\frac{A_{PV}}{A_0} = Q_W^p \left[\frac{\varepsilon (G_E^{p\gamma})^2 + \tau (G_M^{p\gamma})^2}{\varepsilon (G_E^{p\gamma})^2 + \tau (G_M^{p\gamma})^2} \right] + \left[(-1) \frac{\varepsilon G_E^{p\gamma} G_E^{n\gamma} + \tau G_M^{p\gamma} G_M^{n\gamma}}{\varepsilon (G_E^{p\gamma})^2 + \tau (G_M^{p\gamma})^2} \right] + \left[(-1) \frac{(1 - 4 \sin^2 \theta_W) \varepsilon' G_M^{p\gamma} G_A^e}{\varepsilon (G_E^{p\gamma})^2 + \tau (G_M^{p\gamma})^2} \right]. \quad (1.2.10)$$

The reduced asymmetry can be expressed as a combination of three asymmetries as following

$$\frac{A_{PV}}{A_0} = A_{Q-weak} + A_{hadronic} + A_{axial}. \quad (1.2.11)$$

Here individual asymmetries are given as

$$A_{Q-weak} = Q_W^p, \quad (1.2.12)$$

$$A_{hadronic} = Q_W^n \left[\frac{\varepsilon G_E^{p\gamma} G_E^{n\gamma} + \tau G_M^{p\gamma} G_M^{n\gamma}}{\varepsilon (G_E^{p\gamma})^2 + \tau (G_M^{p\gamma})^2} \right], \quad (1.2.13)$$

$$A_{axial} = -G_A^e \left[\frac{(1 - 4 \sin^2 \theta_W) \varepsilon' G_M^{p\gamma}}{\varepsilon (G_E^{p\gamma})^2 + \tau (G_M^{p\gamma})^2} \right], \quad (1.2.14)$$

where the contribution from the strange form factors is ignored.

Under the kinematic condition of $\theta \rightarrow 0$, $\varepsilon \rightarrow 1$, and $\tau \ll 1$, the asymmetry simplifies as

$$\frac{A_{PV}}{A_0} = Q_W^p + Q^2 B(Q^2, \theta), \quad (1.2.15)$$

where the $B(Q^2, \theta)$ term contains the hadronic contribution to the asymmetry and is about 30%.

Previous PVES experiments constrain this contribution.

The goal of the Q-weak experiment is aimed to measure this parity violating asymmetry (~ 250 ppb) in elastic electron-proton scattering at $Q^2 = 0.025$ (GeV/c)² and forward angles to determine the proton's weak charge with 4% combined statistical and systematic uncertainties [8]. The experiment will also provide a $\sim 0.3\%$ measurement of the weak mixing angle. A 2200 hours measurement using a 88% polarized electron beam of 180 μ A on a 35 cm liquid Hydrogen target was performed during 2010 - 2012.

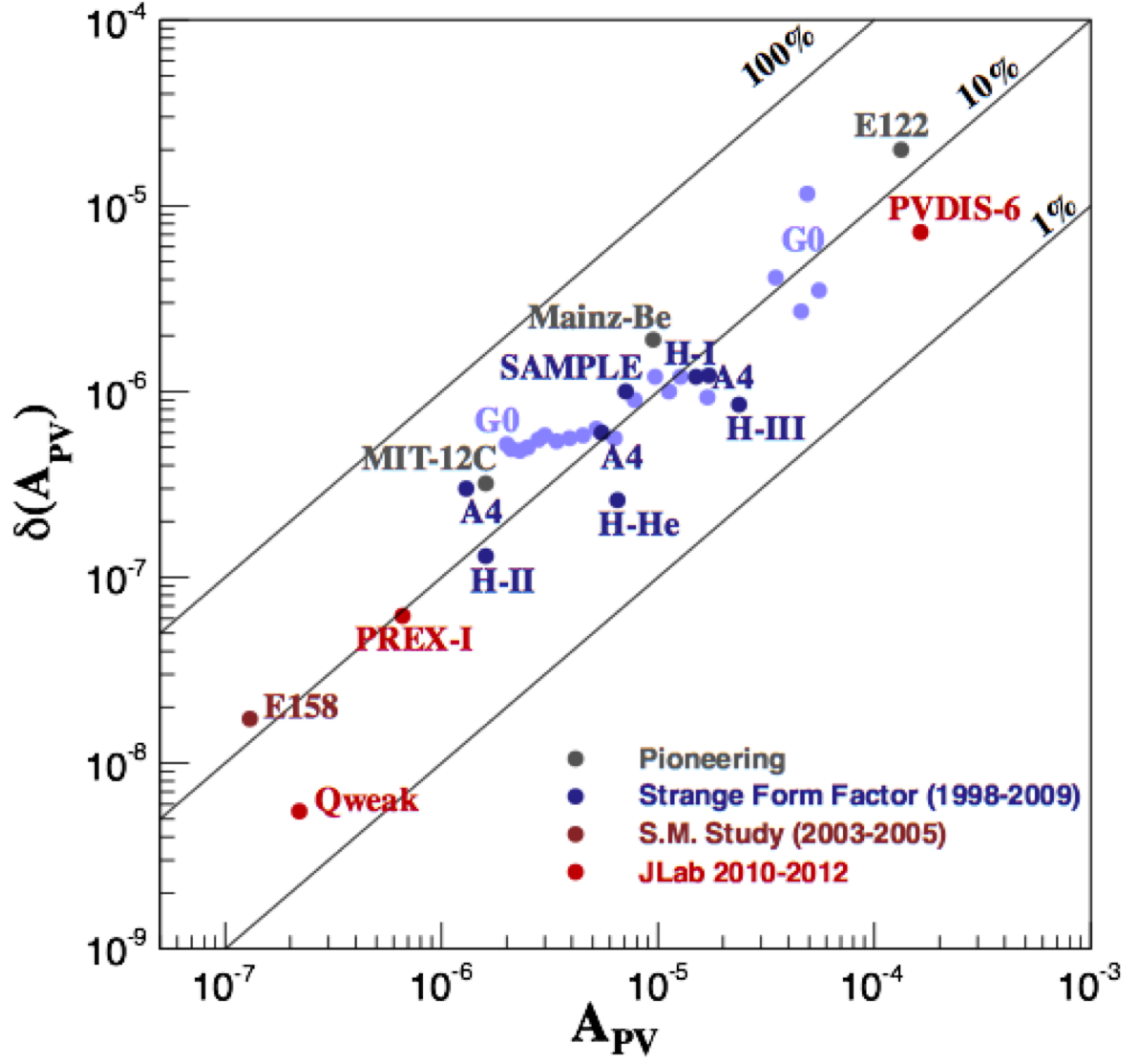


Figure 1.3 Q-weak will be most precise (relative and absolute) PVES result to date.

1.3 Inelastic Parity Violating Asymmetry

In addition of measuring the elastic PV asymmetry for the Q-weak, a dedicated data were taken to extract the inelastic PV asymmetry in electron-proton scattering. During normal production running, the detector signals were integrated to obtain the yield and inelastic events also make into the detector acceptance. There is no clear way to separate the inelastic signal from the elastic signal. The inelastic asymmetry is expected to be a factor of 10 larger than the elastic asymmetry and hence was critical to measure the inelastic dilution and correct for it. The inelastic contribution in the Q-weak acceptance is mainly dominated by the production of the resonance.

1.3.1 The Δ Resonance

The Δ is the first resonance of the nucleon with nucleon spin $J=3/2$ and mass 1232 MeV. In the ground state, the total spin of the proton is $J=1/2$ and is the sum of the spins of its constituent quarks (uud). The nucleon has two valance quark spins aligned parallel and one antiparallel, and hence only two possible flavor states (uud, udd) exist corresponding to isospin 1/2, whereas the Δ baryons have all three quark spins aligned parallel [9]. A list of allowed Δ resonance states and their properties is given in Table 1.2.

Table 1.2 Nucleons and Δ resonances and their associated properties.

Particle	Quarks	EM Charge	Spin	Isopin	I_3
p	uud	+1	$\uparrow\uparrow\downarrow$	1/2	+1/2
n	udd	0	$\uparrow\downarrow\downarrow$	1/2	-1/2
Δ^{++}	uuu	+2	$\uparrow\uparrow\uparrow$	3/2	+3/2
Δ^+	uud	+1	$\uparrow\uparrow\uparrow$	3/2	+1/2
Δ^0	udd	0	$\uparrow\uparrow\uparrow$	3/2	-1/2
Δ^-	ddd	-1	$\uparrow\uparrow\uparrow$	3/2	-3/2

A photon or Z boson can interact with a nucleon and flip the spin of one of the quarks to make them all parallel to produce a Δ baryon. Only a Δ^+ or Δ^0 can be created by this kind of interaction if the target particle is a proton or neutron, respectively. On the other hand, weakly interacting particle, such as a neutrino, a quark can change flavor and flip the spin to produce Δ^{++} and Δ^- . An electron-proton interaction induces a quark spin flip and can reveal information about how the quark spin is redistributed during the transition. For the Q-weak experiment where the interactions were predominantly electron-proton, only the relevant resonance Δ^+ is considered.

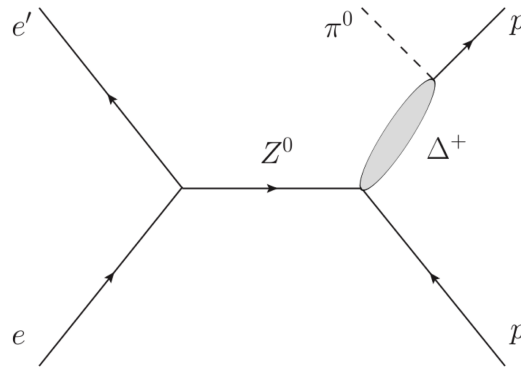


Figure 1.4 The Feynman diagrams for the parity violating inelastic electron-proton scattering [10].

1.3.2 Formalism and Measurement

In inelastic PV electron-proton scattering, the incident electron interacts with the proton and loses energy. The proton absorbs this energy and get excited to its first resonance (Δ^+), then decays to a neutral pion (π^0) and a proton (as shown in Figure 1.4). The parity-violating asymmetry in the nucleon $\rightarrow \Delta$ transition can be expressed as [11, 12]

$$A_{PV}^{in} = \left[\frac{-G_F Q^2}{4\sqrt{2}\pi\alpha} \right] \left[\Delta_{(1)}^\pi + \Delta_{(2)}^\pi + \Delta_{(3)}^\pi \right], \quad (1.3.1)$$

where $\Delta_{(1)}^\pi$ contains the resonant terms, which are all isovector, $\Delta_{(2)}^\pi$ contains the nonresonant terms including both isovector and isoscalar, and $\Delta_{(3)}^\pi$ contains all axial-vector reactions at the hadron vertex. The contribution of the inelastic PV to the Q-weak asymmetry is small. The asymmetry for the $N \rightarrow \Delta$ transition was measured as a part of the Q-weak background studies.

1.4 The Beam Normal Single Spin Asymmetry

The beam normal single spin asymmetry (BNSSA) is generated by polarized electrons when scattered from unpolarized protons and is a possible false background asymmetry in parity violating electron scattering experiments (PVES). The BNSSA is a parity conserving asymmetry. Theoretical calculations [13] indicates that, the size of this asymmetry can be several orders of magnitude larger than that of the parity violating asymmetry. For a precision experiment like Q-weak, it was important to estimate the background due to BNSSA and a dedicated measurement was performed.

Elastic electron-nucleon scattering in the one-photon exchange approximation gives a direct access to the electromagnetic form factors of the nucleon which contains information about its structure. The ratio of the proton's electric to magnetic form factors (G_{Ep}/G_{Mp}) has been measured precisely up to large momentum transfer (Q^2) in precision experiments using two different methods namely the polarization transfer [14, 15] and unpolarized measurements [16–18] using the Rosenbluth separation technique. These two different methods shows inconsistent result. This puzzle may be explained by a two-photon exchange amplitude whose magnitude is a few percent of the one photon exchange term as shown in [19]. A beam normal single spin asymmetry measurement provides a direct access to the two-photon exchange process which is required to properly estimate the electron-nucleon scattering cross-sections beyond the Born approximation.

1.5 Inelastic Beam Normal Single Spin Asymmetry

There is a parity conserving BNSSA or transverse asymmetry (B_n) on H_2 with a $\sin(\phi)$ -like dependence due to 2-photon exchange. The size of B_n is few ppm, so a few percent residual transverse polarization in the beam, in addition to potentially small broken azimuthal asymmetries in the main detector, might lead to few ppb corrections to the Q-weak data. As part of a program of B_n background studies, the first measurement of B_n in the N-to- Δ transition was performed using the Q-weak apparatus.

1.6 Thesis Outline

This dissertation will present a preliminary analysis of the beam normal single spin asymmetry measured from inelastic electron-proton scattering using the Q-weak apparatus. The outline of this dissertation is organized as follows:

- chapter 1: INTRODUCTION - an introduction and motivation for the Q-weak experiment,
- chapter 2: THEORY - an brief overview of the theory of beam normal single spin asymmetry measurements,
- chapter ??: EXPERIMENTAL SETUP - a brief description of the experimental apparatus,
- chapter ??: BEAM MODULATION - provides a detailed description of the beam modulation system,
- chapter ??: BEAMLINE OPTICS AND FALSE ASYMMETRIES - application of beam modulation system, beamline characterization, and pedestal survey,
- chapter ??: BEAM NORMAL SINGLE SPIN ASYMMETRY - gives details of the data analysis and treatment of systematic uncertainties of beam normal single spin asymmetry in inelastic e+p scattering,
- chapter 3: DISCUSSION AND CONCLUSIONS - a summary of the emphasized work and analysis status.

SECTION 2

THEORY

The electromagnetic form factors depict the non-local nature of the nucleon in its interactions with photons. The form factors have been studied extensively both experimentally and theoretically as the basic observables of the nucleon compositeness [20]. Increased precision of electron-proton scattering experiments allowed to extract the form factors precisely and using two alternative methods: the Rosenbluth method - also known as the longitudinal-transverse separation technique [16, 21, 22], and the polarization-transfer technique [14, 15]. The two methods show incompatible results by considering traditional one-photon exchange approximation, called the Born approximation, to extract the form factors. It is important to find an explanation of this discrepancy for the use of the electron-proton scattering as a precise and reliable tool in hadronic physics. Theoretical studies [23, 24] have indicated that the discrepancy could be partially resolved by including higher-order two-photon exchange corrections in the analysis in addition to the lowest-order one-photon exchange approximation. The calculation in Ref. [23] for the two-photon exchange diagrams considered only nucleons in the intermediate state. The Δ resonance has an important role in many hadronic reactions and is essential to evaluate its contribution to the two-photon exchange in electron-proton scattering.

2.1 Electron Scattering Beyond the Born Approximation

Beyond the Born approximation, the calculation of the amplitude of the scattering process becomes very complicated. Two or more photons are exchanged in the scattering process and the calculation gets complex as it needs to include all of the excited states of the proton. There are several existing models to calculate multi-photon processes [25], but they are incomplete.

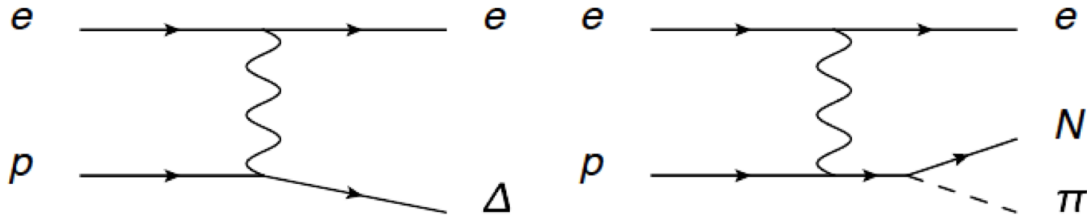


Figure 2.1 Electron-proton \rightarrow electron- Δ in Δ region, without and with decay of Δ in the final state for the one-photon exchange process.

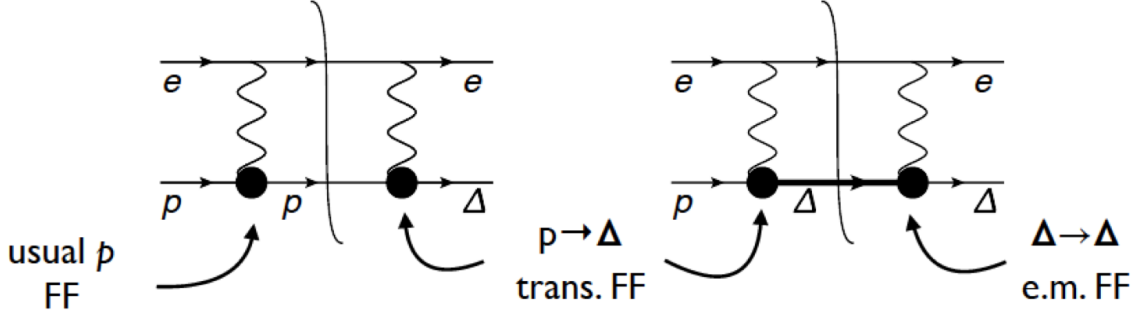


Figure 2.2 BNSSA $2\gamma \Delta$.

2.1.1 2-photon Exchange

The elastic electron-protons scattering at leading order involves the exchange of a single photon, followed by higher-order processes such as two-photon exchange (as shown in Figures 2.1 and 2.2). Elastic electron-protons scattering in Born approximation is usually approximated as a one-photon exchange process. This approximation is possible due to the small value of the electromagnetic coupling constant $\alpha \sim 1/137$. The higher order processes, such as two-photon exchange, are treated as radiative corrections. The two-photon exchange process involves the exchange of two virtual photons with an intermediate hadronic state that includes the ground state and all excited states. The two-photon exchange reactions are used to extract information on the hadron structure such as the form factors of the neutron, pion and heavy nuclei (deuteron and ^3He). In the analysis of the form-factor for electron-proton scattering, the contribution of the two-photon exchange amplitude is assumed to be very small [26]. The real part (or dispersive) of this amplitude is obtained by comparing electron-proton and positron-proton scattering cross sections. The calculations of the two-photon amplitude can be divided into two categories: unexcited and excited intermediate proton states. The effects on the elastic electron-proton scattering cross section of the two-photon exchange contribution with an intermediate Δ resonance is smaller in magnitude than the nucleon contribution [20].

The discrepancy between Rosenbluth separation and the polarization transfer technique using one-photon exchange approximation are shown in Figure 2.3 (a) [27]. The methods start to deviate from each other above Q^2 of 1 $(\text{GeV}/c)^2$. After applying the two-photon exchange correction, the discrepancy seems to be resolved between the two methods, as shown in Figure 2.3 (b) [27]. The two-photon exchange calculations are not complete and have not been tested over a wider range of kinematics.

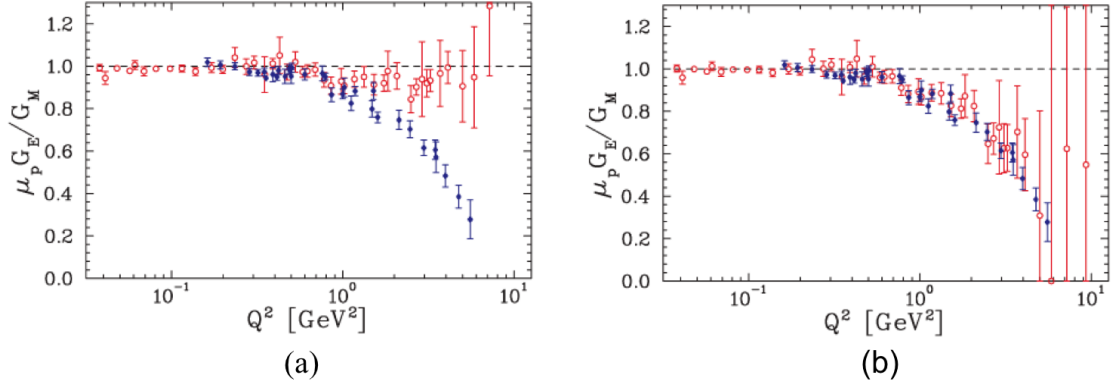


Figure 2.3 Ratio $\mu_p G_E / G_M$ extracted from the polarization transfer (filled diamonds) and LT measurements (open circles). The figure (a) and (b) shows LT separations without and with the two-photon exchange corrections applied to the cross sections respectively.

Another question naturally arises whether other higher-mass resonances could also have a non-negligible contribution to the two-photon exchange correction like $\Delta(1232)$ resonance [13]. The effects turn out to be not too sensitive, as shown by Kondratyuk and Blunden [28] by generalizing the calculation to full spectrum of the most important hadron resonances as intermediate states involving spin 1/2 and 3/2 resonances.

2.2 Experimental Observation of Beam Spin Asymmetry

The beam spin asymmetries are time-reversal invariant, parity conserving observables which vanish in the Born approximation. The beam spin asymmetry can be extracted by observing only the electron in the final state interaction on the electron side (as shown in Figures 2.1 and 2.2). Since one-photon amplitude is real, only imaginary part of the two-photon amplitude contributes to the beam spin asymmetry. The asymmetry arises due to an electron helicity flip. The asymmetry can be obtained either by polarizing the target perpendicular (transverse) to the incoming unpolarized electron beam, or to the transversely polarized beam on a unpolarized target. The asymmetry in the first case is known as target normal single spin asymmetry (A_n) and latter case is called beam normal single spin asymmetry (B_n). The measured asymmetry can be expressed as

$$\epsilon_M = \frac{\sigma^\uparrow - \sigma^\downarrow}{\sigma^\uparrow + \sigma^\downarrow} = \frac{\Im \left[\frac{\sum_{spins} (\mathcal{M}^\gamma)^* (Abs \mathcal{M}^\gamma)}{\sum_{spins} |\mathcal{M}^\gamma|^2} \right]}{1}, \quad (2.2.1)$$

where $\sigma^{\uparrow,\downarrow}$ are cross sections with incoming electrons polarized up or down, perpendicular to the scattering plane. \Im is the imaginary part and $Abs\mathcal{M}^{\gamma\gamma}$ is a sum over all the possible intermediate states in the two-photon exchange process. The cross section can be parameterized using six invariant amplitudes $\tilde{G}_E(\nu, Q^2)$, $\tilde{G}_M(\nu, Q^2)$, and $\tilde{F}_i(\nu, Q^2)$ and are complex functions of the Q^2 and ν . Here $\nu = \vec{K} \cdot \vec{P}$, where K and P are the average of the incoming and outgoing four-momenta of the electron and proton respectively [29, 30]. In the Born approximation, the complex electromagnetic form factors become the usual Pauli and Sachs form factors of the nucleon, $\tilde{G}_E(\nu, Q^2) \rightarrow G_E(Q^2)$, $\tilde{G}_M(\nu, Q^2) \rightarrow G_M(Q^2)$, and $\tilde{F}_i(\nu, Q^2) \rightarrow 0$. After Born approximation, using this parameterization, with the virtual photon polarization parameter,

$$\varepsilon = \frac{\nu^2 - M^4\tau(1+\tau)}{\nu^2 + M^4\tau(1+\tau)}, \quad (2.2.2)$$

the beam normal single spin asymmetry can be expressed as [31]

$$B_n = \frac{2m_e}{Q} \sqrt{2\varepsilon(1-\varepsilon)} \sqrt{1 + \frac{1}{\tau} \left(G_M^2 + \frac{\varepsilon}{\tau} G_E^2 \right)^{-1}} \\ \times \left[-\tau G_M \Im \left(\tilde{F}_3 + \frac{1}{1+\tau} \frac{\nu}{M^2} \tilde{F}_5 \right) - G_E \Im \left(\tilde{F}_4 + \frac{1}{1+\tau} \frac{\nu}{M^2} \tilde{F}_5 \right) \right] + \mathcal{O}(e^4), \quad (2.2.3)$$

where as target normal spin asymmetry can be written as

$$A_n = \sqrt{\frac{1\varepsilon(1+\varepsilon)}{\tau}} \left(G_M^2 + \frac{\varepsilon}{\tau} G_E^2 \right)^{-1} \\ \times \left[-G_M \Im \left(\delta\tilde{G}_E + \frac{\nu}{M^2} \tilde{F}_3 \right) + G_E \Im \left(\delta\tilde{G}_M + \frac{2\varepsilon}{1+\varepsilon} \frac{\nu}{M^2} \tilde{F}_3 \right) \right] + \mathcal{O}(e^4). \quad (2.2.4)$$

To polarize an ultra-relativistic particle in the direction normal to its momentum involves a suppression factor m/E , where m is the mass and E is the energy of the particle. The suppression factor for the electron with beam energy in the 1 GeV range is of order $10^{-4} - 10^{-3}$. The resulting beam-normal single spin asymmetry is expected to be of order $10^{-6} - 10^{-5}$, whereas the target-normal spin asymmetry is of order 10^{-2} [32].

2.2.1 Measurement of the Beam Normal Single Spin Asymmetry

The beam normal single spin asymmetry (BNSSA) is measured by scattering transversely polarized electrons off of unpolarized nucleons. The measured asymmetry (ϵ_M) has a sinusoidal dependence about the beam axis

$$\epsilon_M(\phi) = -B_n \vec{S} \cdot \hat{n} = -B_n |\vec{S}| \sin(\phi - \phi_0), \quad (2.2.5)$$

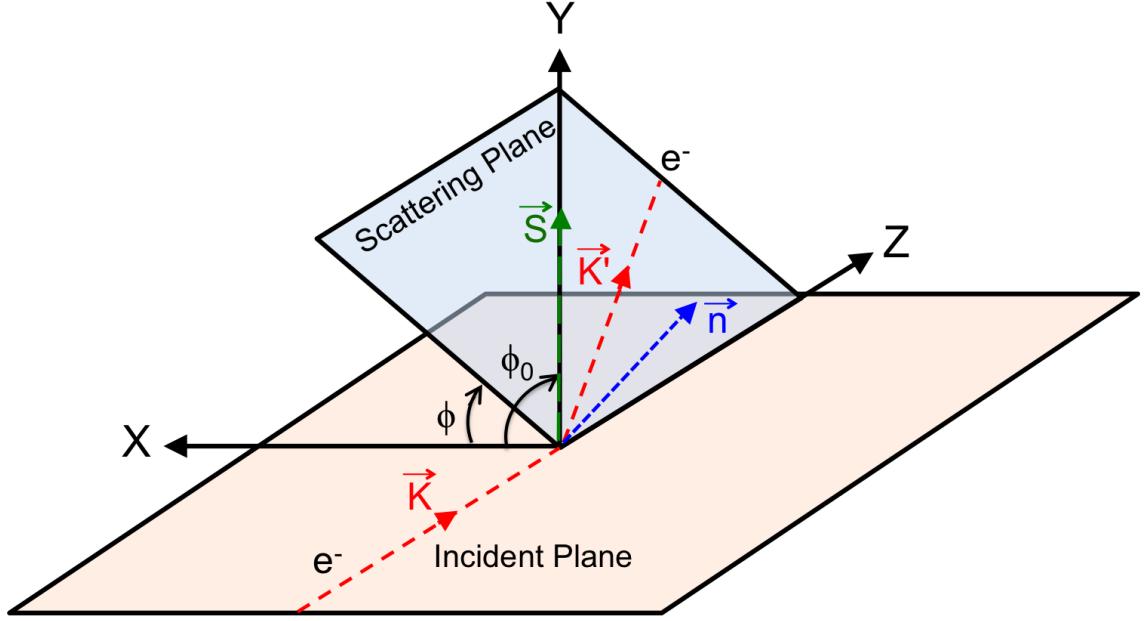


Figure 2.4 The schematic of transverse electron-nucleon scattering reaction. The electron spin is polarized in the vertical transverse direction. The initial (final) momentum of the electron is given by \vec{K} (\vec{K}').

where \vec{S} is the electron spin in the transverse direction, and \hat{n} is the unit vector, normal to the scattering plane. ϕ and ϕ_0 are the azimuthal angles of \vec{S} and the scattering plane respectively (see Figure 2.4). The beam normal single spin asymmetry can be measured and extracted from the asymmetry measured in the detector placing at azimuthal angle ϕ .

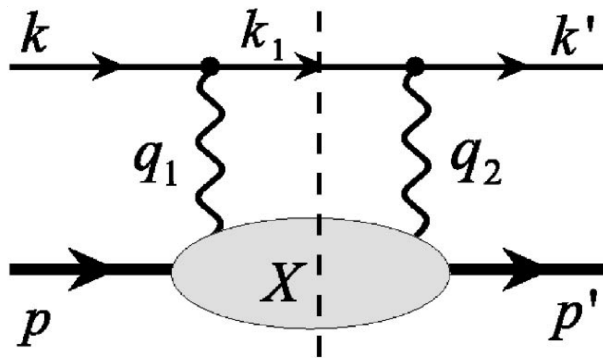


Figure 2.5 The two-photon exchange diagram. The filled blob represents the response of the nucleon to the scattering of the virtual photon [33, 34].

2.2.2 Imaginary Part of Two-photon Diagram

The imaginary part of the two-photon exchange amplitude is related to the absorptive part of the doubly virtual Compton scattering (DVCS) tensor on the nucleon, as shown in Figure 2.5 and can be written as [35]

$$Abs\mathcal{M}^{\gamma\gamma} = e^4 \int \frac{|\vec{k}_1|^2 d|\vec{k}_1| d\Omega_{k_1}}{2E_{k_1} (2\pi)^3} \bar{u}(k') \gamma_\mu (\gamma k_1 + m_e) \gamma_\nu u(k) \frac{1}{Q_1^2 Q_2^2} W^{\mu\nu}(w, Q_1^2, Q_2^2) \quad (2.2.6)$$

The inelastic contribution to $W^{\mu\nu}$ corresponding with the πN intermediate states in the blob of Figure 2.5 using the MAID model (resonance region) [35] is given by

$$W^{\mu\nu}(p', \lambda'_N; p, \lambda_N) = \frac{1}{4\pi^2} \frac{|\vec{p}_\pi|^2}{[|\vec{p}_\pi|(E_\pi + E_n) + E_\pi |\vec{k}_1| \hat{k}_1 \cdot \hat{p}_\pi]} \times \sum_{\lambda_n} \int d\Omega_\pi \bar{u}(p', \lambda'_N) J_{\pi N}^{\dagger\mu} u(p_n, \lambda_n) \times \bar{u}(p_n, \lambda_n) J_{\pi N}^\nu u(p, \lambda_N) \quad (2.2.7)$$

where $p_\pi = (E_\pi, \vec{p}_\pi)$ and $p_n = (E_n, \vec{p}_n)$ are the four-momenta of the intermediate pion and nucleon states, respectively, and $k_1 = -\vec{p}_\pi - \vec{p}_n$. The integration runs over the polar and azimuthal angles of the intermediate pion, and $J_{\pi N}^\nu$ and $J_{\pi N}^{\dagger\mu}$ are the pion electro-production currents, describing the excitation and deexcitation of the πN intermediate state, respectively. u and \bar{u} are matrix elements and can be parameterized. The inelastic contribution is dominated by the region of pion production threshold.

2.3 The $\gamma^* \Delta \Delta$ Form Factors

The proton electromagnetic form factor is well known. The proton $\rightarrow \Delta$ electromagnetic transition form factor is also fairly well known. For proton and Δ intermediate hadrons, vertices therefore are known except for $\gamma^* \Delta \Delta$ electromagnetic vertex. The information about $\gamma^* \Delta \Delta$ form factor has potential to measure charge radius of Δ and magnetic moment of Δ . Besides there have been many theoretical interest:

- Dyson-Schwinger approach [36]
- Covariant quark model [37]
- Lattice QCD [38]

But the form factor experimentally has never been measured before. No dedicated calculations exists to relate $\gamma^* \Delta \Delta$ form factors to cross section or asymmetry data.

2.4 Model Calculations

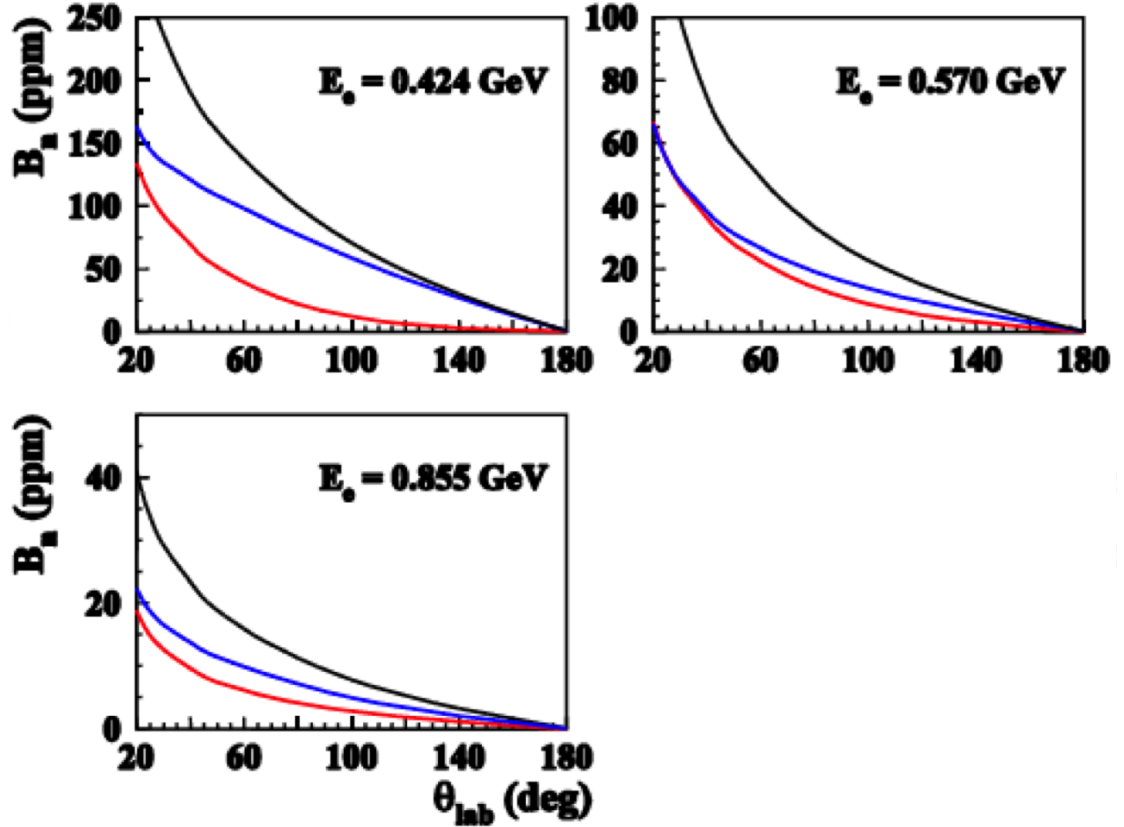


Figure 2.6 Inelastic transverse asymmetry model from Pasquini et al. [39]. Δ intermediate state is shown in red, N intermediate state is shown in blue, and total (Δ +N) contribution is shown in black.

The only unpublished model calculation of the beam normal single spin asymmetry in inelastic electron-nucleon scattering was performed by Pasquini & Vanderhaeghen for forward angles and low energies. The BNSSA as a function of the center-of-mass angle, θ_{cm} for Δ (red) and nucleon (blue) as intermediate states are shown in Figure 2.6. If the intermediate hadronic states are not included in the calculation, the prediction is nearly flat as a function of the θ_{cm} . This calculation was performed for lower energy than Q-weak, and an effort to extrapolate this result in to the Q-weak kinematic settings is discussed in later chapter. The beam normal single spin asymmetry are positive and are in the order of few ppm. The large asymmetries in the forward region dominated by quasi-virtual Compton scattering kinematics, where one exchanged photon becomes quasi-real. The asymmetry almost exponentially varies with scattering angle.

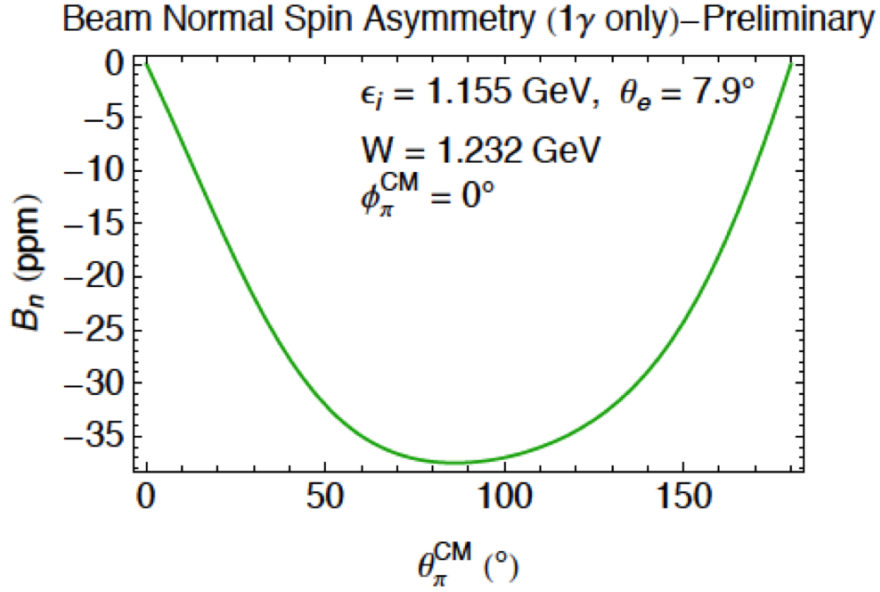


Figure 2.7 Beam normal single spin asymmetry with decay of Δ in the final state for one-photon exchange.

There is an ongoing calculation for one-photon exchange in Δ region [40], which shows the beam normal spin asymmetry is not zero, although is proportional to m_e/Q . The asymmetry is proportional to $\cos\phi_\pi$, the azimuthal angle of the emerging pion relative to the scattering plane. Considering Δ as stable state in $e+p \rightarrow e+\Delta$, one can prove the helicity amplitudes are relatively real, and get $B_n = 0$ [40]. The Δ state decays and final state interaction (FSI) gives different phases for different amplitudes. The phases, and whole amplitudes in FSI are known. The multipole amplitudes can be obtained from analyses of other $e+p \rightarrow e\pi N$ reactions and observing hadronic final state. The variation on B_n with scattering angle is shown in Figure 2.7 [40] by considering only one-photon exchange.

2.5 Goals of the Inelastic Transverse Physics Program

The objective of the Q-weak experiment is to challenge the predictions of the Standard Model in low Q^2 range and search for new physics at the TeV scale through a 4% measurement of the weak charge of the proton via the parity-violating asymmetry (~ 250 ppb) in elastic $e+p$ scattering [8]. There is a parity conserving beam normal single spin asymmetry, or transverse asymmetry, B_n on LH₂ with a $\sin(\phi)$ -like dependence due to the two-photon exchange. The expected magnitude of B_n is few ppm which is an order larger than PV asymmetry for the Q-weak. Also B_n provides

direct access to the imaginary part of the two-photon exchange amplitude. It will be interesting to see the magnitude of B_n in the $N \rightarrow \Delta$ region, which has never been measured before. B_n from electron-nucleon scattering is also a unique tool to study the $\gamma^* \Delta \Delta$ form factors. This dissertation presents the analysis of the 9% measurement of the beam normal single spin asymmetry in inelastic electron-proton scattering at a Q^2 of 0.0209 (GeV/c)^2 . This measurement will help to improve the theoretical models on the beam normal single spin asymmetry and thereby our understanding of the doubly virtual Compton scattering process.

SECTION 3

DISCUSSION AND CONCLUSIONS

3.1 Summary of Results

This dissertation presents the highlights of my Ph.D. research work in the context of the Q-weak experiment. This chapter summarizes the results and conclusions presented so far.

3.2 Contribution Towards Q-weak Experiment

My contributions to the Q-weak experiment towards the measurement of the weak charge of the proton can be summarized under three categories: beam modulation system, beamline optics and false asymmetries, and the beam normal single spin asymmetry measurement in inelastic electron-proton scattering. The experience gained during this experiment will help future precision parity violating measurement at the Jefferson Lab such as the Møller experiment [41].

3.2.1 Beam Modulation

The electron-proton scattering rate largely depends on the five beam parameters: horizontal position, horizontal angle, vertical position, vertical angle, and energy. Changes in these beam parameters when the beam polarization is reversed create false asymmetries. Although attempt has been made to keep changes in beam parameters during reversal as small as possible, it is necessary to correct for such false asymmetries. To make this correction precisely, a beam modulation system was implemented to induce small position, angle, and energy changes at the target to characterize detector response to the beam jitter. The beam modulation system modulated position and angle using two pairs of air-core dipoles separated by ~ 10 m and pulsing one pair at a time to produce relatively pure position or angle changes at the target. The beam energy was modulated using an SRF cavity. The system has been commissioned using the simulated optics from OptiM [42] and collected data during the experiment. The beam modulation system was designed for sinusoidal modulation up to 250 Hz which was robust and well-suited for experiments measuring small parity violating asymmetries like the Q-weak experiment. At the cost of 1% of beam time for one parameter, the system was able to measure all sensitivities to 10% accuracy each day. The pairs of coils were tuned to deliver relatively pure positions or angle modulations, making it much less likely that singular matrices are encountered when solving for the sensitivities. The ratio of coil currents was

adjusted to incorporate any optics change in the beamline compare to move the coils physically, which made the system independent of the design optic. For 1.165 GeV electron beam, using 125 Hz sinusoidal drive signal, the Trim power amplifier was able to provide the desired beam modulation amplitudes with existing air-core MAT coils. The modulation system worked quite well for the span of two years during the Q-weak experiment and collected data noninvasively with production running. Preliminary detector sensitivities were extracted which helped to reduce the width of the measured asymmetry. The beam modulation system also has proven valuable for tracking changes in the optics, such as dispersion at the target and beam position coupling [43]. The system has also helped to track some of the problems in the BPMs in the Hall-C beamline.

3.2.2 Beamline Work

The beam position monitors (BPMs) in front of the target were used for the linear regression and hence was necessary to know their position and angle resolutions. The position resolution of the BPM in front of the target were extracted by observing the residual of beam position differences (between two helicity states) on any BPM and the orbit projected from the virtual target BPM. The concept of the virtual BPM was developed and simulated to determine the position and angle at the target. Using selective data samples from the commissioning phase of the experiment the average BPM resolution was $0.70\text{ }\mu\text{m}$ and $0.77\text{ }\mu\text{m}$ for X and Y respectively. The target BPM angle resolution was simulated using OptiM [42]. A relatively pure position measurement, which corresponds to pure angle measurement at target, was chosen to be at BPM 3P02A from the simulation to extract the angle resolution. Assuming $0.90\text{ (}0.96\text{)}\text{ }\mu\text{m}$ X(Y)-position resolutions, the estimated target BPM angle resolutions at $180\text{ }\mu\text{A}$ are $0.048\text{ }\mu\text{rad}$, and $0.060\text{ }\mu\text{rad}$ for X' and Y' respectively. A new least square linear regression scheme was developed based on this BPM study.

The helicity correlated pedestals were surveyed to improve the false asymmetry contribution for the entire data set of the experiment. No helicity correlated pickups were seen for most of the detector channels and were at $\mathcal{O}(1)$ ppb. Electronic noise levels were generally acceptable, though potentially marginal for the upstream luminosity (USLumi) monitor channels near the end of Run-I but improved during Run-II. Nonlinearity for main detectors were extremely small whereas, USLumi had a nonlinearity of few percent. There is a scope for improvement in USLumi pedestal. Nonlinearity could be very large for low-yield production running on aluminum and $N \rightarrow \Delta$ but still be under 1%. Resolutions for all the detectors were reasonably stable.

3.2.3 Beam Normal Single Spin Asymmetry in Inelastic e+p Scattering

The objective of the Q-weak experiment is to challenge the predictions of the Standard Model in low Q^2 range and search for new physics at the TeV scale through a 4% measurement of the weak charge of the proton via the parity-violating asymmetry (~ 250 ppb) in elastic electron-proton scattering [8]. One of the important correction for the PV asymmetry comes from the residual transverse polarization in the beam. There is a parity conserving beam normal single spin asymmetry or transverse asymmetry (B_n) on H_2 with a $\sin(\phi)$ like dependence due to two-photon exchange. The size of B_n is few ppm. So, a few percent residual transverse polarization in the beam, in addition to potentially small broken azimuthal symmetries in the detector, might lead to few ppb corrections to the Q-weak data. As part of a program of B_n background studies, we made the first measurement of B_n in the $N \rightarrow \Delta$ transition using the Q-weak apparatus. B_n provides direct access to the imaginary part of the two-photon exchange amplitude. The magnitude of B_n in the $N \rightarrow \Delta$ transition has never been measured before. B_n from electron-nucleon scattering is also a unique tool to study the $\gamma^* \Delta \Delta$ form factors [44].

The Q-weak collaboration has made the first measurement of the beam normal single spin asymmetry as $B_n = 42.27 \pm 2.45$ (stat) ± 15.73 (sys) ppm using transversely polarized 1.155 GeV electrons scattering in-elastically from protons with a Q^2 of 0.0209 (GeV/c) 2 . This measurement would be an excellent test of theoretical calculations. In addition to the inelastic data from the proton, Q-weak has data on the B_n measurements from several other physics processes. The asymmetries were measured on liquid hydrogen cell, 4% thick downstream aluminum alloy, and a 1.6% thick downstream carbon foil. Few of these measurements are the first of their kind and carry interesting physics. The analysis of these data is ongoing and expected to test the theoretical models on beam normal single spin asymmetry and thereby our understanding of the doubly virtual Compton scattering process. Unfortunately, at the time of this analysis, there was no existing theoretical calculation or model to compare with the data. Hopefully this thesis will encourage theoreticians to produce new calculations.

REFERENCES

- [1] Francis Halzen and Alan D. Martin. *Quarks and Leptones: An Introductory Course in Modern Particle Physics*. John Wiley and Sons, Inc., 1st edition, January 1984. (Cited on page 1.)
- [2] C.Y. Prescott, W.B. Atwood, R.L.A. Cottrell, H. DeStaebler, Edward L. Garwin, A. Gonnidec, R.H. Miller, L.S. Rochester, T. Sato, D.J. Sherden, C.K. Sinclair, S. Stein, R.E. Taylor, J.E. Clendenin, V.W. Hughes, N. Sasao, K.P. Schler, M.G. Borghini, K. Lbelsmeyer, and W. Jentschke. Parity non-conservation in inelastic electron scattering. *Physics Letters B*, 77(3):347 – 352, 1978. (Cited on page 1.)
- [3] F.J. Hasert, S. Kabe, W. Krenz, J. Von Krogh, D. Lanske, J. Morfin, K. Schultze, H. Weerts, G.H. Bertrand-Coremans, J. Sacton, W. Van Doninck, P. Vilain, U. Camerini, D.C. Cundy, R. Baldi, I. Danilchenko, W.F. Fry, D. Haidt, S. Natali, P. Musset, B. Osculati, R. Palmer, J.B.M. Pattison, D.H. Perkins, A. Pullia, A. Rousset, W. Venus, H. Wachsmuth, V. Brisson, B. Degrange, M. Haguenaue, L. Kluberg, U. Nguyen-Khac, P. Petiau, E. Belotti, S. Bonetti, D. Cavalli, C. Conta, E. Fiorini, M. Rollier, B. Aubert, D. Blum, L.M. Chounet, P. Heusse, A. Lagarrigue, A.M. Lutz, A. Orkin-Lecourtois, J.P. Vialle, F.W. Bullock, M.J. Esten, T.W. Jones, J. McKenzie, A.G. Michette, G. Myatt, and W.G. Scott. Observation of neutrino-like interactions without muon or electron in the gargamelle neutrino experiment. *Physics Letters B*, 46(1):138 – 140, 1973. (Cited on page 1.)
- [4] F.J. Hasert, H. Faissner, W. Krenz, J. Von Krogh, D. Lanske, J. Morfin, K. Schultze, H. Weerts, G.H. Bertrand-Coremans, J. Lemonne, J. Sacton, W. Van Doninck, P. Vilain, C. Baltay, D.C. Cundy, D. Haidt, M. Jaffre, P. Musset, A. Pullia, S. Natali, J.B.M. Pattison, D.H. Perkins, A. Rousset, W. Venus, H.W. Wachsmuth, V. Brisson, B. Degrange, M. Haguenaue, L. Kluberg, U. Nguyen-Khac, P. Petiau, E. Bellotti, S. Bonetti, D. Cavalli, C. Conta, E. Fiorini, M. Rollier, B. Aubert, L.M. Chounet, P. Heusse, A. Lagarrigue, A.M. Lutz, J.P. Vialle, F.W. Bullock, M.J. Esten, T. Jones, J. McKenzie, A.G. Michette, G. Myatt, J. Pinfold, and W.G. Scott. Search for elastic muon-neutrino electron scattering. *Physics Letters B*, 46(1):121 – 124, 1973. (Cited on page 1.)
- [5] F.J. Hasert, S. Kabe, W. Krenz, J. Von Krogh, D. Lanske, J. Morfin, K. Schultze, H. Weerts, G. Bertrand-Coremans, J. Sacton, W. Van Doninck, P. Vilain, R. Baldi, U. Camerini, D.C. Cundy, I. Danilchenko, W.F. Fry, D. Haidt, S. Natali, P. Musset, B. Osculati, R. Palmer,

- J.B.M. Pattison, D.H. Perkins, A. Pullia, A. Rousset, W. Venus, H. Wachsmuth, V. Brisson, B. Degrange, M. Haguenauer, L. Kluberg, U. Nguyen-Khac, P. Petiau, E. Bellotti, S. Bonetti, D. Cavalli, C. Conta, E. Fiorini, M. Rollier, B. Aubert, D. Blum, L.M. Chounet, P. Heusse, A. Lagarrigue, A.M. Lutz, A. Orkin-Lecourtois, J.P. Vialle, F.W. Bullock, M.J. Esten, T.W. Jones, J. McKenzie, A.G. Michette, G. Myatt, and W.G. Scott. Observation of neutrino-like interactions without muon or electron in the gargamelle neutrino experiment. *Nuclear Physics B*, 73(1):1 – 22, 1974. (Cited on page 1.)
- [6] MissMJ. Standard model of elementary particles. (free to use, original file created by user) Own work by uploader, PBS NOVA, Fermilab, Office of Science, United States Department of Energy, Particle Data Group. Licensed under Creative Commons Attribution 3.0 via Wikimedia Commons -http://commons.wikimedia.org/wiki/File:Standard_Model_of_Elementary_Particles.svg#mediaviewer/File:Standard_Model_of_Elementary_Particles.svg, 2014. (Cited on page 2.)
- [7] G. W. Bennett, B. Bousquet, H. N. Brown, G. Bunce, R. M. Carey, P. Cushman, G. T. Danby, P. T. Debevec, M. Deile, H. Deng, S. K. Dhawan, V. P. Druzhinin, L. Duong, F. J. M. Farley, G. V. Fedotovitch, F. E. Gray, D. Grigoriev, M. Grosse-Perdekamp, A. Grossmann, M. F. Hare, D. W. Hertzog, X. Huang, V. W. Hughes, M. Iwasaki, K. Jungmann, D. Kawall, and B. I. Khazin. Measurement of the negative muon anomalous magnetic moment to 0.7 ppm. *Phys. Rev. Lett.*, 92(16):161802, Apr 2004. (Cited on page 1.)
- [8] Q weak Collaboration. The Q-weak Experiment: "A Search for New Physics at the TeV Scale via a Measurement of the Proton's Weak Charge". Technical Report E05-008 Jeopardy proposal, December 2007. (Cited on pages 4, 5, 17, and 21.)
- [9] E. Klempt. Baryon resonances and strong QCD. 2002. (Cited on page 7.)
- [10] John Leacock. *Measuring the Weak Charge of the Proton and the Hadronic Parity Violation of the $N \rightarrow \Delta$ Transition*. PhD thesis, Virginia Polytechnic Institute & State University, Blacksburg, VA 24061-0002, USA, October 2012. (Cited on page 7.)
- [11] Nimai C. Mukhopadhyay, M.J. Ramsey-Musolf, Steven J. Pollock, Jn Lu, and H.-W. Hammer. Parity-violating excitation of the $\delta(1232)$: hadron structure and new physics. *Nuclear Physics A*, 633(3):481 – 518, 1998. (Cited on page 8.)

- [12] Shi-Lin Zhu, C. M. Maekawa, G. Sacco, B. R. Holstein, and M. J. Ramsey-Musolf. Electroweak radiative corrections to parity-violating electroexcitation of the δ . *Phys. Rev. D*, 65:033001, Dec 2001. (Cited on page 8.)
- [13] J. Arrington, P.G. Blunden, and W. Melnitchouk. Review of two-photon exchange in electron scattering. *Progress in Particle and Nuclear Physics*, 66(4):782 – 833, 2011. (Cited on pages 8 and 12.)
- [14] M. K. Jones, K. A. Aniol, F. T. Baker, J. Berthot, P. Y. Bertin, W. Bertozzi, A. Besson, L. Bimbot, W. U. Boeglin, E. J. Brash, D. Brown, J. R. Calarco, L. S. Cardman, C.-C. Chang, J.-P. Chen, E. Chudakov, S. Churchwell, E. Cisbani, D. S. Dale, R. De Leo, A. Deur, B. Diederich, J. J. Domingo, M. B. Epstein, L. A. Ewell, K. G. Fissum, A. Fleck, H. Fonvieille, S. Frullani, J. Gao, F. Garibaldi, A. Gasparian, G. Gerstner, S. Gilad, R. Gilman, A. Glamazdin, C. Glashausser, J. Gomez, V. Gorbenko, A. Green, J.-O. Hansen, C. R. Howell, G. M. Huber, M. Iodice, C. W. de Jager, S. Jaminion, X. Jiang, W. Kahl, J. J. Kelly, M. Khayat, L. H. Kramer, G. Kumbartzki, M. Kuss, E. Lakuriki, G. Lavessière, J. J. LeRose, M. Liang, R. A. Lindgren, N. Liyanage, G. J. Lolos, R. Macri, R. Madey, S. Malov, D. J. Margaziotis, P. Markowitz, K. McCormick, J. I. McIntyre, R. L. J. van der Meer, R. Michaels, B. D. Milbrath, J. Y. Mougey, S. K. Nanda, E. A. J. M. Offermann, Z. Papandreou, C. F. Perdrisat, G. G. Petratos, N. M. Piskunov, R. I. Pomatsalyuk, D. L. Prout, V. Punjabi, G. Quémener, R. D. Ransome, B. A. Raue, Y. Roblin, R. Roche, G. Rutledge, P. M. Rutt, A. Saha, T. Saito, A. J. Sarty, T. P. Smith, P. Sorokin, S. Strauch, R. Suleiman, K. Takahashi, J. A. Templon, L. Todor, P. E. Ulmer, G. M. Urciuoli, P. Vernin, B. Vlahovic, H. Voskanyan, K. Wijesooriya, B. B. Wojtsekhowski, R. J. Woo, F. Xiong, G. D. Zainea, and Z.-L. Zhou. g_{Ep}/g_{Mp} ratio by polarization transfer in e(pol.) p \rightarrow e p(pol.). *Phys. Rev. Lett.*, 84:1398–1402, Feb 2000. (Cited on pages 8 and 10.)
- [15] O. Gayou, K. A. Aniol, T. Averett, F. Benmokhtar, W. Bertozzi, L. Bimbot, E. J. Brash, J. R. Calarco, C. Cavata, Z. Chai, C.-C. Chang, T. Chang, J.-P. Chen, E. Chudakov, R. De Leo, S. Dieterich, R. Endres, M. B. Epstein, S. Escoffier, K. G. Fissum, H. Fonvieille, S. Frullani, J. Gao, F. Garibaldi, S. Gilad, R. Gilman, A. Glamazdin, C. Glashausser, J. Gomez, V. Gorbenko, J.-O. Hansen, D. W. Higinbotham, G. M. Huber, M. Iodice, C. W. de Jager, X. Jiang, M. K. Jones, J. J. Kelly, M. Khandaker, A. Kozlov, K. M. Kramer, G. Kumbartzki, J. J. LeRose, D. Lhuillier, R. A. Lindgren, N. Liyanage, G. J. Lolos, D. J. Margaziotis, F. Marie, P. Markowitz, K. McCormick, R. Michaels, B. D. Milbrath, S. K. Nanda, D. Neyret, Z. Papan-

- dreou, L. Pentchev, C. F. Perdrisat, N. M. Piskunov, V. Punjabi, T. Pussieux, G. Quémener, R. D. Ransome, B. A. Raue, R. Roché, M. Rvachev, A. Saha, C. Salgado, S. Širca, I. Sitnik, S. Strauch, L. Todor, E. Tomasi-Gustafsson, G. M. Urciuoli, H. Voskanyan, K. Wijesooriya, B. B. Wojtsekhowski, X. Zheng, and L. Zhu. Measurement of G_{E_p}/G_{M_p} in $e(\text{pol})p \rightarrow e p(\text{pol})$ to $q^2 = 5.6 \text{ geV}^2$. *Phys. Rev. Lett.*, 88:092301, Feb 2002. (Cited on pages 8 and 10.)
- [16] L. Andivahis, P. E. Bosted, A. Lung, L. M. Stuart, J. Alster, R. G. Arnold, C. C. Chang, F. S. Dietrich, W. Dodge, R. Gearhart, J. Gomez, K. A. Griffioen, R. S. Hicks, C. E. Hyde-Wright, C. Keppel, S. E. Kuhn, J. Lichtenstadt, R. A. Miskimen, G. A. Peterson, G. G. Petratos, S. E. Rock, S. Rokni, W. K. Sakumoto, M. Spengos, K. Swartz, Z. Szalata, and L. H. Tao. Measurements of the electric and magnetic form factors of the proton from $q^2=1.75$ to $8.83 (\text{geV}/c)^2$. *Phys. Rev. D*, 50:5491–5517, Nov 1994. (Cited on pages 8 and 10.)
- [17] M. E. Christy, A. Ahmidouch, C. S. Armstrong, J. Arrington, R. Asaturyan, S. Avery, O. K. Baker, D. H. Beck, H. P. Blok, C. W. Bochna, W. Boeglin, P. Bosted, M. Bouwhuis, H. Breuer, D. S. Brown, A. Bruell, R. D. Carlini, N. S. Chant, A. Cochran, L. Cole, S. Danagoulian, D. B. Day, J. Dunne, D. Dutta, R. Ent, H. C. Fenker, B. Fox, L. Gan, H. Gao, K. Garrow, D. Gaskell, A. Gasparian, D. F. Geesaman, P. L. J. Guèye, M. Harvey, R. J. Holt, X. Jiang, C. E. Keppel, E. Kinney, Y. Liang, W. Lorenzon, A. Lung, P. Markowitz, J. W. Martin, K. McIlhany, D. McKee, D. Meekins, M. A. Miller, R. G. Milner, J. H. Mitchell, H. Mkrtchyan, B. A. Mueller, A. Nathan, G. Niculescu, I. Niculescu, T. G. O'Neill, V. Papavassiliou, S. F. Pate, R. B. Piercey, D. Potterveld, R. D. Ransome, J. Reinhold, E. Rollinde, P. Roos, A. J. Sarty, R. Sawafta, E. C. Schulte, E. Segbefia, C. Smith, S. Stepanyan, S. Strauch, V. Tadevosyan, L. Tang, R. Tieulent, A. Uzzle, W. F. Vulcan, S. A. Wood, F. Xiong, L. Yuan, M. Zeier, B. Zihlmann, and V. Ziskin. Measurements of electron-proton elastic cross sections for $0.4 < Q^2 < 5.5 (\text{GeV}c)^2$. *Phys. Rev. C*, 70:015206, Jul 2004. (Cited on page 8.)
- [18] J. Arrington. New measurement of $G(E) / G(M)$ for the proton. 2003. (Cited on page 8.)
- [19] P. A. M. Guichon and M. Vanderhaeghen. How to reconcile the rosenbluth and the polarization transfer methods in the measurement of the proton form factors. *Phys. Rev. Lett.*, 91:142303, Oct 2003. (Cited on page 8.)
- [20] S. Kondratyuk, P. G. Blunden, W. Melnitchouk, and J. A. Tjon. δ resonance contribution to two-photon exchange in electron-proton scattering. *Phys. Rev. Lett.*, 95:172503, Oct 2005. (Cited on pages 10 and 11.)

- [21] R. C. Walker, B. W. Filippone, J. Jourdan, R. Milner, R. McKeown, D. Potterveld, L. Andivahis, R. Arnold, D. Benton, P. Bosted, G. deChambrier, A. Lung, S. E. Rock, Z. M. Szalata, A. Para, F. Dietrich, K. Van Bibber, J. Button-Shafer, B. Debebe, R. S. Hicks, S. Dasu, P. de Barbaro, A. Bodek, H. Harada, M. W. Krasny, K. Lang, E. M. Riordan, R. Gearhart, L. W. Whitlow, and J. Alster. Measurements of the proton elastic form factors for $1 \leq Q^2 \leq 3$ (gev/c)² at slac. *Phys. Rev. D*, 49:5671–5689, Jun 1994. (Cited on page 10.)
- [22] I. A. Qattan, J. Arrington, R. E. Segel, X. Zheng, K. Aniol, O. K. Baker, R. Beams, E. J. Brash, J. Calarco, A. Camsonne, J.-P. Chen, M. E. Christy, D. Dutta, R. Ent, S. Frullani, D. Gaskell, O. Gayou, R. Gilman, C. Glashauser, K. Hafidi, J.-O. Hansen, D. W. Higinbotham, W. Hinton, R. J. Holt, G. M. Huber, H. Ibrahim, L. Jisonna, M. K. Jones, C. E. Keppel, E. Kinney, G. J. Kumbartzki, A. Lung, D. J. Margaziotis, K. McCormick, D. Meekins, R. Michaels, P. Monaghan, P. Moussiegt, L. Pentchev, C. Perdrisat, V. Punjabi, R. Ransome, J. Reinhold, B. Reitz, A. Saha, A. Sarty, E. C. Schulte, K. Slifer, P. Solvignon, V. Sulkosky, K. Wijesooriya, and B. Zeidman. Precision rosenbluth measurement of the proton elastic form factors. *Phys. Rev. Lett.*, 94:142301, Apr 2005. (Cited on page 10.)
- [23] P. G. Blunden, W. Melnitchouk, and J. A. Tjon. Two-photon exchange and elastic electron-proton scattering. *Phys. Rev. Lett.*, 91:142304, Oct 2003. (Cited on page 10.)
- [24] S. Kondratyuk, P.G. Blunden, W. Melnitchouk, and J.A. Tjon. Two-photon exchange in elastic and inelastic electron-proton scattering. *AIP Conf.Proc.*, 842:336–338, 2006. (Cited on page 10.)
- [25] Megh Raj Niroula. *Beyond the Born Approximation: a Precise Comparison of $e+p$ and $e-p$ Elastic Scattering in the CEBAF Large Acceptance Spectrometer (CLAS)*. PhD thesis, Old Dominion University, VA, May 2010. (Cited on page 10.)
- [26] Gary K. Greenhut. Two-photon exchange in electron-proton scattering. *Phys. Rev.*, 184:1860–1867, Aug 1969. (Cited on page 11.)
- [27] J. Arrington, W. Melnitchouk, and J. A. Tjon. Global analysis of proton elastic form factor data with two-photon exchange corrections. *Phys. Rev. C*, 76:035205, Sep 2007. (Cited on page 11.)
- [28] S. Kondratyuk and P. G. Blunden. Contribution of spin 1/2 and 3/2 resonances to two-photon exchange effects in elastic electron-proton scattering. *Phys. Rev. C*, 75:038201, Mar 2007. (Cited on page 12.)

- [29] M. Gorchtein, P.A.M. Guichon, and M. Vanderhaeghen. Normal spin asymmetries in elastic electron-proton scattering. *Nuclear Physics A*, 755(0):273 – 276, 2005. Proceedings of the 10th International Conference on the Structure of Baryons. (Cited on page 13.)
- [30] Juliette Mammei. *Parity-Violating Elastic Electron Nucleon Scattering: Measurement of the Strange Quark Content of the Nucleon and Towards a Measurement of the Weak Charge of the Proton*. PhD thesis, Virginia Polytechnic Institute & State University, Blacksburg, VA 24061-0002, USA, April 2010. (Cited on page 13.)
- [31] M Gorchtein, P.A.M Guichon, and M Vanderhaeghen. Beam normal spin asymmetry in elastic lepton-nucleon scattering. *Nuclear Physics A*, 741(0):234 – 248, 2004. (Cited on page 13.)
- [32] Carl E. Carlson and Marc Vanderhaeghen. Two-photon physics in hadronic processes. *Annual Review of Nuclear and Particle Science*, 57(1):171–204, 2007. (Cited on page 13.)
- [33] B. Pasquini and M. Vanderhaeghen. Resonance estimates for single spin asymmetries in elastic electron-nucleon scattering. *Phys. Rev. C*, 70:045206, Oct 2004. (Cited on page 14.)
- [34] B. Pasquini and M. Vanderhaeghen. Single spin asymmetries in elastic electron-nucleon scattering. *Eur Phys J*, 24:29–32, 2005. (Cited on page 14.)
- [35] M. Gorchtein. Beam normal spin asymmetry in the quasisreal compton scattering approximation. *Phys. Rev. C*, 73:055201, May 2006. (Cited on page 15.)
- [36] Jorge Segovia, Chen Chen, IanC. Clot, CraigD. Roberts, SebastianM. Schmidt, and Shaolong Wan. Elastic and transition form factors of the delta(1232). *Few-Body Systems*, 55(1):1–33, 2014. (Cited on page 15.)
- [37] G. Ramalho, M. T. Peña, and A. Stadler. Shape of the δ baryon in a covariant spectator quark model. *Phys. Rev. D*, 86:093022, Nov 2012. (Cited on page 15.)
- [38] Constantia Alexandrou, Tomasz Korzec, Giannis Koutsou, Cdric Lorc, John W. Negele, Vladimir Pascalutsa, Antonios Tsapalis, and Marc Vanderhaeghen. Quark transverse charge densities in the from lattice {QCD}. *Nuclear Physics A*, 825(1-2):115 – 144, 2009. (Cited on page 15.)
- [39] Barbara Pasquini. Two-Photon Physics: Theory. MAMI and Beyond: <http://wwwkph.kph.uni-mainz.de/T//MAMIandBeyond/02%20Dienstag/08%20Pasquini.pdf>, April 2009. (Cited on page 16.)

- [40] Carl Carlson. BSA.N Δ @Qweak. <https://qweak.jlab.org/doc-private/ShowDocument?docid=2060>, August 2014. (Cited on page 17.)
- [41] K. Kumar *et al.* The MOLLER Experiment: Measurement Of Lepton Lepton Elastic Reactions. <http://hallaweb.jlab.org/collab/PAC/PAC37/C12-09-005-Moller.pdf>, December 2010. (Cited on page 19.)
- [42] Valery Lebedev. OPTIM: Computer code for linear and non-linear optics calculations. <http://www-bdnew.fnal.gov/pbar/organizationalchart/lebedev/OptiM/optim.htm>, June 2007. (Cited on pages 19 and 20.)
- [43] Nuruzzaman and Qweak Collaboration. Beam modulation system for the q-weak experiment at jefferson lab. *AIP Conference Proceedings*, 1560(1):240–242, 2013. (Cited on page 20.)
- [44] Constantia Alexandrou, Tomasz Korzec, Giannis Koutsou, Cedric Lorce, John W. Negele, et al. Quark transverse charge densities in the *Delta*(1232) from lattice QCD. *Nucl.Phys.*, A825:115–144, 2009. (Cited on page 21.)